

Synthesis of Hydride and Alkyl Compounds Containing the Cp*Os(NO) Fragment. Crystal Structure of [Cp*Os(μ -NO)]₂

Julia L. Brumaghim, James G. Priepot, and Gregory S. Girolami*

School of Chemical Sciences, University of Illinois at Urbana–Champaign,
600 South Mathews Avenue, Urbana, Illinois 61801

Received July 30, 1998

Treatment of the pentamethylcyclopentadienyl (Cp*) compound Cp*Os(NO)Br₂ (**1**) with NaBH₄ yields the dihydride Cp*Os(NO)H₂. The dihydride loses H₂ over several days in solution to form [Cp*Os(μ -NO)]₂; this dinuclear compound can also be formed directly by reduction of **1** with zinc powder. The X-ray crystal structure of [Cp*Os(μ -NO)]₂ shows that nitrosyl ligands are bridging and that the Os–Os distance is 2.539(1) Å. Compound **1** reacts with MgR₂ to form the monoalkylated products Cp*Os(NO)RBr, where R = Me, CH₂SiMe₃, Ph, or *o*-Tol. The slow ligand substitution kinetics of this reaction prevent the formation of dialkyls of stoichiometry Cp*Os(NO)R₂, even after long reaction times or when a large excess of alkylating agent is used. Dialkyls such as Cp*Os(NO)Me₂ can, however, be obtained by treatment of Cp*Os(NO)MeBr with silver trifluoromethanesulfonate followed by addition of dimethylmagnesium.

Introduction

The nitric oxide molecule occupies a unique place in transition metal chemistry because it is the only strong π -acceptor with “ambi-valent” character.^{1,2} In particular, group 8 metal complexes of the formula Cp*M(NO)L₂ engage in many interesting reactions, both with and without the direct involvement of the nitrosyl ligand. One well-studied reaction of Cp*M(NO)L₂ complexes is migratory insertion of the nitrosyl ligand into a metal–alkyl bond. For example, treatment of Cp*Fe(NO)Me₂ with PMe₃ affords the nitrosoalkane complex Cp*Fe(NOMe)Me(PMe₃).³ The corresponding Cp*Ru(NO)R₂ complexes (R = Me, Et) undergo similar migratory insertion reactions as an intermediate step in forming oximate, cyano, and carboxamide products.^{4,5}

In most cases, however, the NO group in Cp*M(NO)L₂ complexes serves as a spectator ligand. For example, the water-soluble dication [Cp*Ru(NO)(dppz)]²⁺, where dppz = dipyrrodo(3,2-*a*:2',3'-*c*)phenazine, has been found to intercalate into and promote the photolytic cleavage of one strand of supercoiled DNA.⁶ The Cp*Ru(NO)²⁺ fragment is stable in aqueous solutions, and the aqua complex [Cp*Ru(NO)(H₂O)]²⁺ has been characterized by X-ray crystallography. Dissolution of this complex in D₂O causes complete deuteration of the Cp* methyl groups.⁷

Several Cp*M(NO)L₂ complexes are able to undergo insertion reactions that result in the formation of C–C bonds. For example, the cationic alkyl complex [Cp*Ru(NO)Me(H₂O)]⁺ reacts with methyl acrylate to form a chelated methyl insertion product.⁸ In a similar manner, the triflate complexes Cp*Ru(NO)R(O₃SCF₃), where R = Me or Ph, react with diphenylacetylene to yield ruthenacyclopentadiene complexes formed from insertion of the alkyne into the Ru–R bond followed by orthometalation of a phenyl group.⁹

Another class of C–C bond forming reactions exhibited by Cp*M(NO)L₂ complexes are those that involve reductive elimination. Thermolysis of the iron bis(benzyl) complex Cp*Fe(NO)(CH₂C₆H₅)₂ affords dibenzyl and the dinuclear complex [Cp*Fe(NO)]₂.¹⁰ The analogous ruthenium bis(aryl) complexes Cp*Ru(NO)R₂, where R is phenyl or *p*-tolyl, react similarly in ethanol, acetonitrile, or 1,2-dichloroethane to produce diaryl and [Cp*Ru(NO)]₂.^{11,12} Interestingly, carrying out the thermolysis of Cp*Ru(NO)R₂ in hexane generates a different product, [Cp*Ru(NO)R]₂,^{11–13} and in CH₂Cl₂ the haloalkyl complex Cp*Ru(NO)Cl(CH₂Cl) is formed.¹² Carbon–carbon bond formation of a different kind is exhibited by the chloromethyl complex Cp*Ru(NO)(CH₂Cl)₂. Thermolysis or photolysis of this compound results in formation of ethylene and the dichloride Cp*Ru(NO)Cl₂.¹⁴

(1) Richter-Addo, G. B.; Legzdins, P. *Chem. Rev.* **1988**, *88*, 991–1010.

(2) Mingos, D. M. P.; Sherman, D. J. *Adv. Inorg. Chem.* **1989**, *34*, 293–375.

(3) Seidler, M. D.; Bergman, R. G. *Organometallics* **1983**, *2*, 1897–1899.

(4) Chang, J.; Seidler, M. D.; Bergman, R. G. *J. Am. Chem. Soc.* **1989**, *111*, 3258–3271.

(5) Seidler, M. D.; Bergman, R. G. *J. Am. Chem. Soc.* **1984**, *106*, 6110–6111.

(6) Schoch, T. K.; Hubbard, J. L.; Zoch, C. R.; Yi, G.-B.; Sørli, M. *Inorg. Chem.* **1996**, *35*, 4383–4390.

(7) Svetlanova-Larsen, A.; Zoch, C. R.; Hubbard, J. L. *Organometallics* **1996**, *15*, 3076–3087.

(8) Hauptman, E.; Brookhart, M.; Fagan, P. J.; Calabrese, J. C. *Organometallics* **1994**, *13*, 774–780.

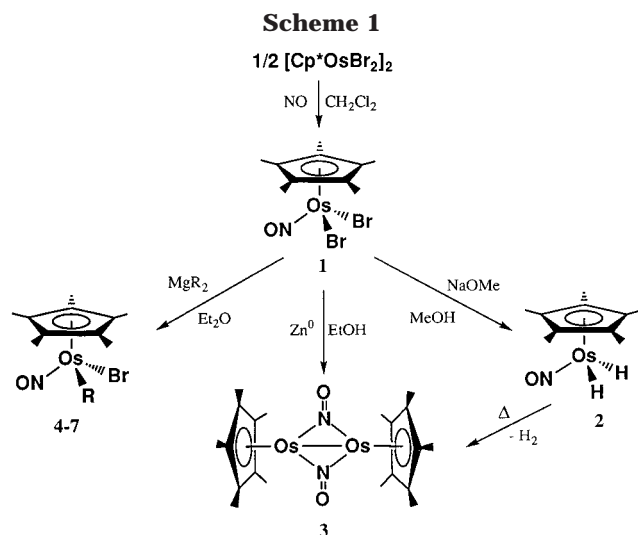
(9) Burns, R. M.; Hubbard, J. L. *J. Am. Chem. Soc.* **1994**, *116*, 9514–9520.

(10) Diel, B. N. *J. Organomet. Chem.* **1985**, *284*, 257–262.

(11) Chang, J.; Bergman, R. G. *J. Am. Chem. Soc.* **1987**, *109*, 4298–4304.

(12) Hubbard, J. L.; Morneau, A.; Burns, R. M.; Zoch, C. R. *J. Am. Chem. Soc.* **1991**, *113*, 9176–9180.

(13) Tagge, C. D.; Bergman, R. G. *J. Am. Chem. Soc.* **1996**, *118*, 6908–6915.



The $\text{Cp}^*\text{M}(\text{NO})$ fragment can also bind to arenes. For example, treatment of $\text{Cp}^*\text{Ru}(\text{NO})\text{Me}(\text{OTf})$ with $\text{LiH}\cdot\text{BET}_3$ and naphthalene generates the η^2 -arene complex $\text{Cp}^*\text{Ru}(\text{NO})(\eta^2\text{-naphthalene})$. This arene complex reacts with HSiPh_3 and with aryl disulfides to produce the free naphthalene and corresponding hydrido/silyl and bis-(thiolato) oxidative addition products.¹³

Although complexes that contain $\text{Cp}^*\text{Fe}(\text{NO})$ and $\text{Cp}^*\text{Ru}(\text{NO})$ units have been well-studied, relatively few examples of compounds containing the corresponding $\text{CpOs}(\text{NO})$ or $\text{Cp}^*\text{Os}(\text{NO})$ units have been synthesized. Several $[\text{CpOs}(\text{NO})(\text{PR}_3)_2]^+$ cations were described in 1982;¹⁵ more recently, the polychalcogenide complexes $\text{Cp}^*\text{Os}(\text{NO})(\text{E}_4)$, where $\text{E} = \text{S}$ or Se ,¹⁶ and the ferrocene-linked complex $\text{Cp}^*\text{Os}(\text{NO})(\mu\text{-S})_2(\text{ferrocene})$ have been reported.¹⁷ The latter complexes were prepared from $[\text{Cp}^*\text{OsBr}_2]_2$, a molecule that we described in 1994;¹⁸ treatment of this dinuclear complex with nitric oxide gives the mononuclear nitrosyl complex $\text{Cp}^*\text{Os}(\text{NO})\text{Br}_2$.¹⁹ This latter nitrosyl compound is analogous to the widely used starting material $\text{Cp}^*\text{Ru}(\text{NO})\text{Cl}_2$,^{4,5,12,20} and we now show that it serves as an excellent entry point for the exploration of $\text{Cp}^*\text{Os}(\text{NO})$ chemistry. We describe the synthesis of several $\text{Cp}^*\text{Os}(\text{NO})\text{BrR}$ and $\text{Cp}^*\text{Os}(\text{NO})\text{R}_2$ alkyl and hydride compounds as well as the synthesis and structure of the dinuclear nitrosyl complex $[\text{Cp}^*\text{Os}(\text{NO})]_2$. In many respects, the chemistry of these compounds differs significantly from that of their iron and ruthenium analogues.

Results and Discussion

The reactions described in this paper are summarized in Scheme 1. Physical properties and microanalytical data for the new compounds are given in Table 1. The

(14) Hubbard, J. L.; Morneau, A.; Burns, R. M.; Nadeau, O. W. *J. Am. Chem. Soc.* **1991**, *113*, 9180–9184.

(15) Bruce, M. I.; Tomkins, I. B.; Wong, F. S.; Skelton, B. W.; White, A. H. *J. Chem. Soc., Dalton Trans.* **1982**, 687–692.

(16) Herberhold, M.; Jin, G.-X.; Liable-Sands, L. M.; Rheingold, A. L. *J. Organomet. Chem.* **1996**, *519*, 223–227.

(17) Herberhold, M.; Jin, G.-X.; Trukenbrod, I.; Milius, W. *Z. Anorg. Allg. Chem.* **1996**, *622*, 724–728.

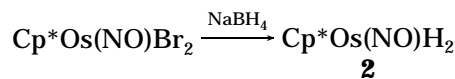
(18) Gross, C. L.; Girolami, G. S.; Wilson, S. R. *J. Am. Chem. Soc.* **1994**, *116*, 10294–10295.

(19) Gross, C. L.; Girolami, G. S. *Organometallics* **1996**, *15*, 5359–5367.

(20) Efraty, A.; Eblaze, G. *J. Organomet. Chem.* **1984**, *260*, 331–334.

^1H and ^{13}C NMR data for these compounds are shown in Table 2. For all the compounds, parent peaks are observable in the mass spectra.

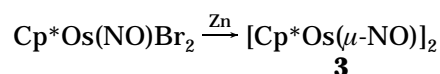
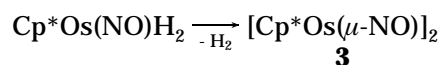
Synthesis and Characterization of $\text{Cp}^*\text{Os}(\text{NO})\text{H}_2$. Treatment of the previously reported^{16,19} compound $\text{Cp}^*\text{Os}(\text{NO})\text{Br}_2$ (**1**) with excess NaBH_4 in ethanol gives the dihydride $\text{Cp}^*\text{Os}(\text{NO})\text{H}_2$ (**2**) in 35–40% yield. This yellow compound is best purified by sublimation at 50 °C in a vacuum.



The ^1H NMR spectrum of **2** features a singlet of relative intensity 2 at $\delta -12.36$ for the hydride ligands, and the IR spectrum contains a ν_{NO} band at 1734 cm^{-1} and a ν_{OSH} band at 2088 cm^{-1} . The frequency of the former band suggests that the nitrosyl ligand is linear, as expected from the valence electron count.

Only a few other group 8 nitrosyl/hydride complexes are known.²¹ For example, the complex $\text{RuH}(\text{NO})(\text{PPh}_3)_3$ is a catalyst for the dimerization of diphenylacetylene.²² The related cations $[\text{OsH}_2(\text{NO})(\text{PPh}_3)_3]^+$ and $[\text{OsH}_2(\text{NO})(\text{CO})(\text{PR}_3)_2]^+$, where $\text{R} = \text{Ph}$ or c-Hx , are the only other group 8 nitrosyl dihydride complexes that have been reported.^{23,24}

Synthesis and Crystal Structure of $[\text{Cp}^*\text{Os}(\mu\text{-NO})]_2$. The dihydride compound **2** darkens in the solid state over a period of 2 days at room temperature and is unstable in solution even at low temperatures. Over a period of weeks in CH_3CN at $-20\text{ }^\circ\text{C}$, compound **2** loses dihydrogen and dimerizes to form a new species, the dinuclear complex $[\text{Cp}^*\text{Os}(\text{NO})]_2$ (**3**). Compound **3** can also be synthesized in 76% yield by the reduction of **1** with zinc powder in refluxing ethanol. The dinuclear nature of the complex is evident from its mass spectrum, which contains a set of peaks near $m/z = 712$.



The ^1H NMR spectrum of **3** confirms that the two Cp^* groups are equivalent, and the IR spectrum contains a strong band at 1405 cm^{-1} , which is assigned to the ν_{NO} stretch. The low frequency of this band (vs 1734 cm^{-1} for the terminal nitrosyl ligand in **2**) suggests that the nitrosyl ligands in **3** bridge the Os–Os bond. The nitrosyl stretching frequency for **3** compares well to those seen for the known iron (1472 cm^{-1})²⁵ and ruthenium (1455 cm^{-1})¹² analogues.

Cyclic voltammetry studies in both dichloromethane and tetrahydrofuran show that **3** undergoes no oxidation or reduction processes between 1.0 and -2.6 V versus Ag/AgCl .

(21) Berke, H.; Burger, P. *Comments Inorg. Chem.* **1994**, *16*, 279–312.

(22) Sanchez-Delgado, R. A.; Wilkinson, G. *J. Chem. Soc., Dalton Trans.* **1977**, 804–809.

(23) Boyar, E. B.; Dobson, A.; Robinson, S. D.; Haymore, B. L.; Huffman, J. C. *J. Chem. Soc., Dalton Trans.* **1985**, 621–627.

(24) Johnson, B. F. G.; Segal, J. A. *J. Chem. Soc., Dalton Trans.* **1974**, 981–984.

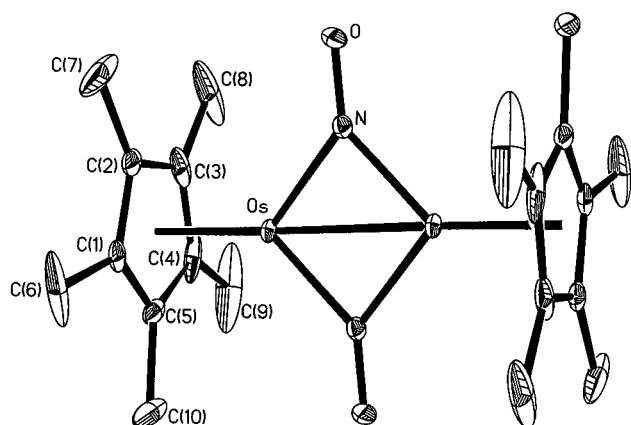
(25) Kubat-Martin, K. A.; Barr, M. E.; Spencer, B.; Dahl, L. F. *Organometallics* **1987**, *6*, 2570–2579.

Table 1. Physical and Microanalytical Data for the New Osmium–Nitrosyl Compounds

compound	mp, °C	ν_{NO} , cm^{-1}	analysis, % ^a		
			C	H	N
Cp*Os(NO)H ₂ (2)	78 (dec)	1734	33.73 (33.59)	4.85 (4.79)	3.76 (3.92)
[Cp*Os(NO)] ₂ (3)	183 (dec)	1405	33.41 (33.79)	4.41 (4.25)	3.70 (3.94)
Cp*Os(NO)MeBr (4)	182	1738	29.64 (29.34)	3.80 (4.03)	3.12 (3.11)
Cp*Os(NO)(CH ₂ SiMe ₃)Br (5)	248 (dec)	1724	32.52 (32.18)	5.44 (5.02)	2.28 (2.68)
Cp*Os(NO)PhBr (6)	252	1740	37.84 (37.50)	3.97 (3.93)	2.57 (2.74)
Cp*Os(NO)(<i>o</i> -Tol)Br (7)	>250	1729	38.85 (38.78)	4.33 (4.21)	2.57 (2.67)

^a Calculated values in parentheses.**Table 2. ¹H and ¹³C{¹H} NMR Data at 25 °C for the New Osmium–Nitrosyl Compounds^a**

cmpd, solvent	¹ H	assgnmt	¹³ C{ ¹ H}	
Cp*Os(NO)H ₂ (2), CH ₂ Cl ₂	2.25 (s)	C ₅ Me ₅	98.4 (s)	
	-12.36 (s)	C ₅ Me ₅	11.5 (s)	
		Os-H		
[Cp*Os(NO)] ₂ (3), CH ₂ Cl ₂	1.83 (s)	C ₅ Me ₅	94.7 (s)	
		C ₅ Me ₅	7.7 (s)	
Cp*Os(NO)MeBr (4), CH ₂ Cl ₂	1.40 (s)	C ₅ Me ₅	101.5 (s)	
	2.16 (s)	C ₅ Me ₅	9.2 (s)	
		Os-Me	-15.5 (s)	
Cp*Os(NO)(CH ₂ SiMe ₃)Br (5), C ₆ D ₆	1.39 (s)	C ₅ Me ₅	101.4 (s)	
	0.36 (s)	C ₅ Me ₅	8.7 (s)	
	2.51 (d, <i>J</i> _{HH} = 10.7)	} CH ₂	2.2 (s)	
	1.80 (d, <i>J</i> _{HH} = 10.9)		-7.0 (s)	
	Cp*Os(NO)PhBr (6), CH ₂ Cl ₂	7.30 (dd, <i>J</i> _{HH} = 7.5, 1.0)	<i>o</i> -CH	142.4 (s)
			<i>ipso</i> -C	134.2 (s)
7.12 (t, <i>J</i> _{HH} = 7.5)		<i>p</i> -CH	128.4 (s)	
7.00 (td, <i>J</i> _{HH} = 7.3, 1.0)		<i>m</i> -CH	125.1 (s)	
		C ₅ Me ₅	104.8 (s)	
		C ₅ Me ₅	10.1 (s)	
		<i>o</i> -CMe	147.5 (s)	
Cp*Os(NO)(<i>o</i> -Tol)Br (7), CH ₂ Cl ₂	7.20 (dd, <i>J</i> _{HH} = 7.4, 1.4)	<i>o</i> -CH	144.9 (s)	
		<i>ipso</i> -C	137.7 (s)	
	7.10 (dd, <i>J</i> _{HH} = 7.1, 1.4)	<i>m</i> -CH	128.8 (s)	
	6.93 (td, <i>J</i> _{HH} = 7.2, 1.6)	<i>m'</i> -CH	125.7 (s)	
	6.88 (td, <i>J</i> _{HH} = 7.3, 1.6)	<i>p</i> -CH	125.3 (s)	
		C ₅ Me ₅	104.9 (s)	
		<i>o</i> -CMe	27.7 (s)	
		C ₅ Me ₅	10.1 (s)	
Cp*Os(NO)Me ₂ (8), C ₆ D ₆	1.38 (s)	C ₅ Me ₅	97.5 (s)	
	1.37 (s)	C ₅ Me ₅	8.4 (s)	
		Os-Me	-18.9 (s)	

^a All chemical shifts are reported in ppm; all coupling constants are reported in Hz.**Figure 1.** Molecular structure of [Cp*Os(NO)]₂, **3**. Ellipsoids are drawn at the 30% probability density level. Hydrogen atoms are omitted for clarity.

The molecular structure of **3** has been determined from a single-crystal X-ray diffraction study (Figure 1); crystallographic data are presented in Table 3, and selected bond lengths and angles given in Table 4. As expected from the IR results, the nitrosyl ligands bridge the two osmium atoms and form a symmetric, planar

Os₂(NO)₂ core. The average Os–N distance is 1.920(6) Å and the N–O distance is 1.249(7) Å. The Os–Os distance of 2.539(1) Å is relatively short²⁶ and is consistent with the Os–Os double bond expected from the electron count of **3**. The crystal structure of the analogous ruthenium compound [Cp*Ru(NO)]₂ has not been reported,¹¹ but the Fe–Fe double-bond distance in [(C₅H₄Me)Fe(NO)]₂ is 2.326(4) Å.²⁵ This metal–metal distance is shorter than that in **3** owing to the smaller radius of Fe. The central Fe₂(NO)₂ core of [(C₅H₄Me)₂Fe(NO)]₂ is also symmetric and planar within experimental error.

The 2.539(1) Å osmium–osmium distance in **3** can be compared with the Os–Os distances in other multiply bonded dimers. For example, Os–Os triple bonds range in length from 2.271(1) to 2.441(1) Å.²⁶ The hydride-bridged Os=Os double-bond length in Cp*₂Os₂(CO)₂H₂ is 2.677(1) Å.²⁷

Synthesis and Characterization of Cp*Os(NO)-RBr and Cp*Os(NO)R₂ Compounds.

(26) Cotton, F. A.; Walton, R. A. *Multiple Bonds between Metal Atoms*, 2nd ed.; Clarendon Press: Oxford, England, 1993.

(27) Hoyano, J. K.; Graham, W. A. G. *J. Am. Chem. Soc.* **1982**, *104*, 3722–3723.

Table 3. Crystal Data Collection and Structural Refinement Parameters for [Cp*Os(μ -NO)]₂ (3)

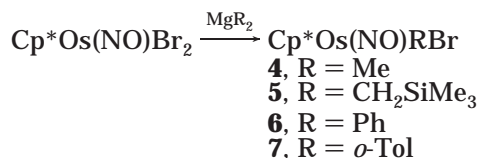
$T = 198(2)$ K	space group: $P2_1/n$
$a = 9.7276(4)$ Å	$V = 1017.10(7)$ Å ³
$b = 7.2584(3)$ Å	$Z = 2$
$c = 14.9069(5)$ Å	mol wt = 710.86
$\alpha = 90^\circ$	$\rho_{\text{calc}} = 2.321$ g cm ⁻³
$\beta = 104.908(1)^\circ$	$\mu = 12.497$ mm ⁻¹
$\gamma = 90^\circ$	size = $0.17 \times 0.1 \times 0.01$ mm
diffractometer: Siemens Smart System	
radiation: Mo K α , $\lambda = 0.710$ 73 Å	
collection range, method: 2.26–28.32°, area detector	
index ranges: $-5 \leq h \leq 12$, $-9 \leq k \leq 9$, $-19 \leq l \leq 19$	
reflns: 6446 total, 2437 unique, 1966 obsd [$I > 2\sigma(I)$]	
abs corr, transm factors: face indexed, 0.275–0.884	
refinement: full-matrix least-squares on F^2	
largest diff peak and hole: 2.15 and -0.99 e Å ⁻³	
$R_2 = 0.0447$	R_1 (obsd data) = 0.0309
no. of parameters = 124	wR_2 (obsd data) = 0.0668
GOF on $F^2 = 1.042$	R_1 (all data) = 0.0463
ext coeff = $1.6(2) \times 10^{-6}$	wR_2 (all data) = 0.0741

Table 4. Selected Bond Distances (Å) and Angles (deg) for [Cp*Os(μ -NO)]₂ (3)

bond distances		bond angles	
Os–Os' ^a	2.5394(4)	Os–N–O	137.4(5)
Os–N	1.925(5)	Os'–N–O	139.8(4)
Os–N'	1.914(6)	N–Os–N'	97.2(2)
N–O	1.249(7)	Os–N–Os'	82.8(2)

^a Primed atoms are related to unprimed atoms by the transformation $-x+1, -y+2, -z$.

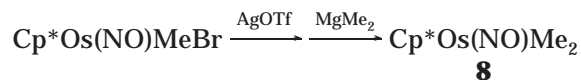
compound **1** with dialkyl- or diarylmagnesium reagents results in the replacement of one bromide ligand and formation of the corresponding Cp*Os(NO)RBr monoalkyls and monoaryls. The NO stretching frequencies of these compounds are shown in Table 1, and NMR data are given in Table 2.



The Cp*Os(NO)RBr compounds **4**–**7** are stable in the presence of both oxygen and water. In addition, these compounds are stable at temperatures greater than 200 °C; compounds **4** and **5** melt without decomposition at 182 and 252 °C, respectively. All of these alkyl and aryl compounds have NO stretching frequencies in the range 1740–1729 cm⁻¹, as is expected for linear nitrosyl groups. The ¹H and ¹³C NMR spectra of these compounds are consistent with the expected structures. For compound **5**, the CH₂ protons in the (trimethylsilyl)methyl ligand are diastereotopic and appear at δ 2.51 and 1.80 in the ¹H NMR spectrum.

Dialkylated products of stoichiometry Cp*Os(NO)R₂ cannot be obtained by addition of dialkylmagnesium agents to Cp*Os(NO)Br₂. Even after long reaction times or when a large excess of alkylating agent is used, only the monoalkylated products are obtained. Organoaluminum reagents are also unable to effect complete alkylation; stirring Cp*Os(NO)Br₂ for 4 days with an excess of AlMe₃ yields only the monoalkylated Cp*Os(NO)MeBr compound. In contrast, treatment of Cp*Os(NO)MeBr with AgOTf in CH₂Cl₂ and then with MgMe₂ in Et₂O affords the dimethyl complex Cp*Os(NO)Me₂

(**8**) in good yield. The ¹H NMR spectrum of **8** shows two singlets at δ 1.38 and 1.37 in a 5:2 ratio for the methyl groups on the Cp* ligand and the osmium, respectively. In the ¹³C{¹H} NMR spectrum, the osmium methyl signal is seen as a singlet at δ –18.9.



Comparison of Osmium, Ruthenium, and Iron Chemistry. Iron, ruthenium, and osmium generally have similar reaction chemistries, but osmium forms stronger bonds and is easier to oxidize.¹⁹ As a result, osmium forms some compounds for which the iron and ruthenium analogues are unknown. The dihydride Cp*Os(NO)H₂, **2**, is one example of this phenomenon: the iron and ruthenium analogues Cp*Fe(NO)H₂ and Cp*Ru(NO)H₂ have never been reported. Owing to the large osmium–hydrogen bond strength²⁸ (and to the electron-donating properties of the Cp* ligand),²⁹ the reductive elimination of H₂ from **2** is slow enough to permit the isolation of this compound at room temperature.

The stronger metal–ligand bonds formed by osmium are also evident from the nitrosyl stretching frequencies. Now that [Cp*Os(NO)]₂ is known, compounds of stoichiometry [Cp*M(NO)]₂ exist for all three group 8 elements. Their ν_{NO} stretching frequencies are 1472 cm⁻¹,²⁵ 1455 cm⁻¹,¹² and 1405 cm⁻¹ for M = Fe, Ru, and Os, respectively. The decrease in the ν_{NO} stretching frequency is consistent with the stronger M–NO backbonding into the NO π^* orbital expected for the heavier transition metal congeners.

In addition, the ligand substitution rates are much slower for osmium than for ruthenium. Specifically, alkylation of Cp*Os(NO)Br₂ with LiMe, MgMe₂, or AlMe₃ generates only trace amounts (at best) of the dimethyl compound Cp*Os(NO)Me₂, and instead only the monoalkyl Cp*Os(NO)MeBr is obtained. Even if the alkylation reactions are carried out for extended times (e.g., 4 days), little or no dialkylated product could be isolated. These results stand in sharp contrast to the facile alkylation reactions seen for the ruthenium analogue Cp*Ru(NO)Cl₂, which reacts with AlMe₃ to afford the dimethyl compound Cp*Ru(NO)Me₂ in about an hour.⁴ In fact, Chang and Bergman report that monoalkylated (or monoarylated) ruthenium compounds of stoichiometry Cp*Ru(NO)RCl could not be prepared by treatment of Cp*Ru(NO)Cl₂ with 1 equiv of an alkylating agent, the dialkyls being obtained instead.¹¹ The only reported example of a monoarylated compound, Cp*Ru(NO)PhCl, was synthesized by protonolysis of the diphenyl compound with HCl.⁴

Thus, the greater kinetic stability of the osmium compounds relative to their ruthenium analogues has both advantages and disadvantages. On one hand, the dihydride Cp*Os(NO)H₂ is kinetically stable enough to isolate; on the other hand, the dialkyls Cp*Os(NO)R₂ cannot be synthesized by direct alkylation of a halide precursor. Instead, these osmium dialkyl complexes must be synthesized by more indirect methods.

(28) Connor, J. A. *Top. Curr. Chem.* **1977**, *71*, 71–110.

(29) See: Gassman, P. G.; Mickelson, J. W.; Sowa, J. R., Jr. *J. Am. Chem. Soc.* **1992**, *114*, 6942–6944, and references therein.

Experimental Section

General Details. All experiments were performed under argon or in a vacuum using standard Schlenk techniques unless otherwise specified. Solvents were distilled under nitrogen from magnesium turnings (ethanol), calcium hydride (dichloromethane), or sodium benzophenone (pentane, ether). Water was deionized before use. Nitric oxide (Union Carbide, MG Industries) and zinc dust (Mallinckrodt) were used without further purification. The dialkylmagnesium reagents were prepared by modifications of a standard route.³⁰ The starting material Cp*Os(NO)Br₂ was prepared by means of the literature method¹⁹ and washed with pentane to remove trace Cp*₂Os impurities.

The IR spectra were obtained on a Nicolet Impact 410 as Nujol mulls between KBr plates. The ¹H and ¹³C NMR data were recorded on Varian Unity-400 spectrometers at 400 and 125 MHz, respectively. Chemical shifts are reported in parts per million (δ) downfield from tetramethylsilane. Field-desorption (FD) mass spectra were performed on a Finnigan-MAT 731 mass spectrometer; the samples were loaded as CH₂Cl₂ solutions, and the spectrometer source temperature was 100 °C. Positive-ion fast-atom bombardment (FAB) mass spectra were performed on a VG ZAB-SE mass spectrometer as CH₂Cl₂ solutions. The shapes of all peak envelopes correspond with those calculated from the natural abundance isotopic distributions. Cyclic voltammograms were obtained on a BAS CV 50W Voltammeter; the supporting electrolyte was [N(*n*-Bu)₄]PF₆, and the working electrode was constructed of platinum. Melting points were measured on a Thomas-Hoover Unimelt apparatus in sealed capillaries under argon. Microanalyses were performed by the staff of the Microanalytical Laboratory of the School of Chemical Sciences at the University of Illinois.

(Pentamethylcyclopentadienyl)nitrosyldihydroosmium(II), Cp*Os(NO)H₂ (2). To a mixture of Cp*Os(NO)Br₂ (0.30 g, 0.59 mmol) and NaBH₄ (0.80 g, 2.1 mmol) was added ethanol (30 mL). Upon addition of the solvent, gas was evolved (H₂), and the solution color became brown. The solution was stirred for 1 h, and then the solvent was removed under vacuum. The resulting residue was extracted with pentane (3 \times 15 mL), and the brown extracts were filtered. The pentane was removed under vacuum, and the resulting solid was sublimed at 10⁻³ Torr over 4 h at 50 °C to afford a yellow solid. Yield: 0.085 g (40%). MS (FD): *m/z* 359 [M⁺]. IR (cm⁻¹): 3375 (w), 2096 (s), 1735 (s), 1070 (m), 1042 (m), 856 (w), 789 (s), 749 (m), 620 (m), 535 (m).

Bis(pentamethylcyclopentadienyl)dinitrosyldiosmium(0), [Cp*Os(μ -NO)]₂ (3). To a suspension of Cp*Os(NO)Br₂ (0.325 g, 0.63 mmol) in ethanol (50 mL) was added zinc dust (0.14 g, 2.1 mmol). The mixture was heated to reflux for 3 h, during which time the purple solution became red. The solvent was removed under vacuum, and the residue was dissolved in tetrahydrofuran (20 mL). The solution was filtered through Celite in air and then concentrated to 5 mL. The red microcrystalline precipitate was collected by filtration and dried under vacuum. Yield: 0.171 g (76%). MS (FD): *m/z* 712 [M⁺]. IR (cm⁻¹): 1408 (s), 1340 (s), 1159 (w), 1069 (m), 702 (s), 610 (w), 581 (m), 440 (w).

(Pentamethylcyclopentadienyl)nitrosyl(methyl)osmium(II), Cp*Os(NO)MeBr (4). To a suspension of Cp*Os(NO)Br₂ (0.30 g, 0.60 mmol) in diethyl ether (35 mL) was added dimethylmagnesium (2.0 mL of a 1.4 M solution in diethyl ether, 2.8 mmol). The purple mixture was stirred for 5 h, during which time the suspension dissolved and the solution color became dark reddish-brown. The solution was washed in air with water (3 \times 20 mL), dried over magnesium sulfate, and filtered. The solution was concentrated to 3 mL

and cooled to -20 °C to afford red-orange crystals. Yield: 0.181 g (79%). MS (FD): *m/z* 451 [M⁺]. IR (cm⁻¹): 3464 (w), 1738 (s), 1208 (m), 1158 (w), 628 (w), 603 (w), 582 (m), 550 (w), 510 (m).

(Pentamethylcyclopentadienyl)nitrosyl[(trimethylsilyl)methyl]bromoosmium(II), Cp*Os(NO)(CH₂SiMe₃)Br (5). The procedure for the synthesis of Cp*Os(NO)MeBr was followed; the reagents used were Cp*Os(NO)Br₂ (0.11 g, 0.20 mmol) and Mg(CH₂SiMe₃)₂ (3 mL of a 0.4 M solution in diethyl ether, 1.20 mmol). Yield: 0.081 g (74%). MS (FD): *m/z* 523 [M⁺]. IR (cm⁻¹): 3414 (w), 1724 (s), 1230 (m), 1239 (m), 1025 (m), 864 (m), 835 (m), 732 (w), 679 (w), 563 (w).

(Pentamethylcyclopentadienyl)nitrosyl(phenyl)bromoosmium(II), Cp*Os(NO)PhBr (6). To a suspension of Cp*Os(NO)Br₂ (0.11 g, 0.20 mmol) in diethyl ether (30 mL) was added diphenylmagnesium (2 mL of a 0.5 M solution in diethyl ether, 1.0 mmol). The purple mixture was stirred for 4 h, during which time the suspension dissolved and the solution color became dark red. The solution was taken to dryness in a vacuum, and the resulting residue was extracted with dichloromethane (30 mL). The extract was washed in air with water (3 \times 20 mL), dried over magnesium sulfate, and filtered. The dichloromethane was removed under vacuum, and the resulting dark red solid was dissolved in tetrahydrofuran (5 mL). The solution was concentrated to ~1 mL, layered with pentane (10 mL), and cooled to -20 °C to afford maroon crystals. Yield: 0.067 g (64%). MS (FAB): *m/z* 513 [M⁺]. IR (cm⁻¹): 3054 (w), 1740 (s), 1566 (m), 1070 (w), 1042 (w), 1020 (m), 750 (s), 708 (m), 508 (w).

(Pentamethylcyclopentadienyl)nitrosyl(o-tolyl)bromoosmium(II), Cp*Os(NO)(o-Tol)Br (7). To a suspension of Cp*Os(NO)Br₂ (0.10 g, 0.20 mmol) in diethyl ether (30 mL) was added di(o-tolyl)magnesium (2.45 mL of a 0.20 M solution in diethyl ether, 0.49 mmol). The purple mixture was stirred for 18 h, during which time the suspension dissolved and the solution color became dark red. The solution was taken to dryness in a vacuum, and the resulting residue was extracted with dichloromethane (30 mL). The extract was washed in air with water (3 \times 20 mL), dried over magnesium sulfate, and filtered. The dichloromethane was removed under vacuum, and the resulting dark red solid was dissolved in tetrahydrofuran (5 mL). The solution was concentrated to ~1 mL, layered with pentane (10 mL), and cooled to -20 °C to afford maroon crystals. Yield: 0.087 g (81%). MS (FAB): *m/z* 527 [M⁺]. IR (cm⁻¹): 1729 (s), 1575 (m), 1161 (w), 1031 (s), 754 (w).

(Pentamethylcyclopentadienyl)nitrosyldimethyl-osmium(II), Cp*Os(NO)Me₂ (8). To a solution of Cp*Os(NO)-MeBr (0.02 g, 0.04 mmol) in dichloromethane (30 mL) was added silver triflate (0.02 g, 0.08 mmol). The solution was stirred for 2.5 h, and a white precipitate formed after 20 min. The yellow solution was filtered, and the filtrate was taken to dryness under vacuum. The resulting yellow solid was dissolved in diethyl ether (30 mL) and treated with dimethylmagnesium (0.5 mL of a 1.4 M solution in diethyl ether, 0.69 mmol). The solution was stirred for 5 h, and then the solvent was removed under vacuum. The residue was extracted with pentane, and the filtrate was taken to dryness under vacuum to yield a yellow solid. MS (FD): 385 *m/z* [M⁺]. IR (cm⁻¹): 1696 (ν_{NO}).

Crystallographic Study. Single crystals of [Cp*Os(μ -NO)]₂, grown from acetonitrile, were mounted on glass fibers with Paratone-N oil (Exxon) and immediately cooled to -75 °C in a cold nitrogen gas stream on the diffractometer. Standard peak search and indexing procedures,³¹ followed by least-squares refinement³¹ using 3425 reflections, yielded the cell dimensions given in Table 3.

Data were collected with an area detector by using the measurement parameters listed in Table 3. Systematic absences for 0*kl* (*k* \neq 2*n*) and *h*0*l* (*h* + 1 \neq 2*n*) were only consistent with space group *P*2₁/*n*. The measured intensities were reduced to structure factor amplitudes and their esd's

(30) Andersen, R. A.; Wilkinson, G. *Inorg. Synth.* **1979**, *19*, 262–265.

by correction for background³¹ and Lorentz³² and polarization³² effects. Although corrections for crystal decay were unnecessary, a face-indexed absorption correction was applied,³¹ the maximum and minimum transmission factors being 0.884 and 0.275. Systematically absent reflections were deleted and symmetry equivalent reflections were averaged to yield the set of unique data. The $\bar{1}01$ reflection was occluded by the beam stop and was therefore omitted from the least-squares refinement. The remaining 2437 data were used in the least-squares refinement.

The correct position for the osmium atom was deduced from a sharpened Patterson map.³¹ Subsequent least-squares refinement and difference Fourier calculations revealed the positions of the remaining non-hydrogen atoms. Hydrogen atoms were placed in "idealized" positions and their locations were optimized by rotation about the C–C bonds with C–H = 0.98 Å. The analytical approximations to the scattering factors were used, and all structure factors were corrected for both the real and imaginary components of anomalous dispersion.³³ Independent anisotropic displacement factors were refined for the nonhydrogen atoms. The displacement factors for the hydrogen atoms were set equal to 1.5 times U_{eq} for the attached carbon atoms. An isotropic extinction parameter was refined to a final value of $x = 1.6(2) \times 10^{-6}$, where F_c is multiplied by the factor $k[1 + F_c^2 x \lambda^3 / \sin 2\theta]^{-1/4}$ with k being the overall scale factor.³⁴ The quantity minimized by the least-

squares program was $\sum w(F_o^2 - F_c^2)^2$, where $w = \{[\sigma(F_o^2)]^2 + (0.0336P)^2 + 2.9862P\}^{-1}$ and $P = (F_o^2 + 2F_c^2)/3$.³¹ Successful convergence was indicated by the maximum shift/error of 0.002 for the last cycle. The largest peak in the final Fourier difference map ($2.1 \text{ e } \text{Å}^{-3}$) was located 0.94 Å from C9. This peak does not necessarily reflect disorder in the Cp* positions because no other significant peaks are present in the difference map. Instead, the coordinates of this peak are almost exactly related to those of the osmium atom by the transformation $x, 1.5-y, z$. It is unclear to us whether this peak reflects systematic errors in the data or a real physical phenomenon (such as a stacking fault), but fortunately this difference peak is relatively small. A final analysis of variance between observed and calculated structure factors showed no apparent errors.

Acknowledgment. We thank the Department of Energy (Grant DEFG02-96-ER45439) for support of this work, and Dr. Scott Wilson and Ms. Teresa Wieckowska of the University of Illinois X-ray Crystallographic Laboratory for collecting the data for **3**. We also thank a referee for encouraging us to develop a method to prepare Cp*Os(NO)Me₂. J.L.B. thanks the University of Illinois for a departmental fellowship.

Supporting Information Available: Tables of atomic coordinates, bond distances and angles, and displacement parameters for **3** are available (5 pages). This material is available free of charge via the Internet at <http://pubs.acs.org>.

OM980657H

(31) Software packages used by the University of Illinois X-ray Crystallographic Laboratory include the following: SMART (Version 4), SAINT (Version 4), and SHELXTL (Version 5), all of which were obtained from Siemens Industrial Automation, Inc., Madison, WI, 1994.

(32) Stout, G. H.; Jensen, J. H. *X-ray Structure Determination, A Practical Guide*, 2nd ed.; Wiley: New York, 1989; pp 178–182.

(33) Creagh, D. C.; McAuley, W. J. In *International Tables for Crystallography*; Wilson, A. J. C., Ed.; Kluwer Academic Publishers: Boston, 1992; Vol. C, pp 206–211.

(34) Zachariasen, W. H. *Acta Crystallogr., Sect. A: Cryst. Phys., Diffraction Theory*. **1968**, *24*, 212–216.